Universitat Autònoma de Barcelona

Facultat de Ciències

Secció de Ciències Ambientals

TESTING THE POTENTIAL OF $^{90}Y/^{90}Sr$ DISEQUILIBRIUM IN ESTIMATING OCEANIC POC EXPORT OVER DAILY TIMESCALES

Viena Puigcorbé Lacueva

Projecte de Fin de Carrera
de Ciències Ambientals

Febrer 2009

Directror: Dr. Pere Masqué Barri

A tots aquells que han contribuït a fer de
mi la persona que sóc avui.

Acknowledgments

Vull agrair molt sincerament a Pere Masqué, director d'aquest treball, l'oportunitat de participar en el seu grup de recerca, tota la confiança que ha dipositat en mi des del primer dia però, sobretot, vull agrair-li que sempre ha estat quan l'he necessitat, fins i tot quan jo mateixa no n'era conscient, fos l'hora que fos. Moltes gràcies.

A en Jordi Garcia per iniciar-me en el món de la radioactivitat ambiental i per pensar en mi a l'hora de buscar algú per una possible incorporació al grup.

Als companys i companyes del Laboratori de Radioactivitat Ambiental (LRA), Ester, Elisabet, Carolina, Núria, Patricia, César i Valentí perquè des del primer dia m'han considerat una més, han comptat amb mi i sempre han estat disposats a donar-me un cop de mà quan m'han vist perduda, sobretot aquests darrers dies. Treballar amb vosaltres és una sort perquè sou un gran grup, acadèmicament i a nivell personal.

Vull agrair especialment a l'Elisabet tot el que he après d'ella. La campanya GoCAL4 va ser una gran experiència i ella va ser una gran mestre i amiga, i segueix sent ambdues coses.

A la Núria per les estones compartides al lab i als ferrocarrils on he pogut explicar les coses que em preocupaven i relativitzar-les gràcies a tu.

A la Carolina per seguir-me ajudant amb els números, tan de bon matí com abans d'anar a dormir, i per animar-me amb les seves preguntes de resposta òbvia en les que '*quien calla otorga'*.

A l'Ester per la seva alegria contagiosa, per ser tot cor i per fer-nos riure tant (nenas nenas nenas....anem al karaoke!), s'agraeix molt en aquests moments.

A en Valentí per reviure amb mi l'època en què ell estava escrivint el projecte i per preguntar-me cada dia com duia el treball. Espero compartir moltes més campanyes com la que vàrem fer (a les pròximes em remullo jo també).

Amb la Patricia i el César no he tingut tanta relació però espero que compartim més hores de laboratori, de despatx, de congrés i/o de festa i que ens coneguem una mica més. Estic segura que puc aprendre molt de vosaltres.

A en Joan Manel Bruach per tot el suport tècnic donat, per ajudar-me amb les comandes per les campanyes (sense tu no sé com m'ho faria) i per trobar els reactius que mai no veig.

A la María Villa que m'ha ajudat des del primer moment amb el projecte. Ella ha estat una peça clau en aquest treball i li estic molt agraïda per tot l'esforç dedicat i per la paciència que ha tingut amb mi. Sé que ha sido duro, muchas gracias.

Thanks to Claudia Benitez-Nelson for making my participation in the GoCAL4 cruise possible, for taking care of me here and there, for her ideas, but overall, for the energy and desire that she transmits. You can never be discouraged with her by your side. Terminaré hablando inglés, ya lo verás.

Gracias a Déborah Simón, Jason Addison, Efrain Wong y Paulina Durazo por los buenos momentos vividos en el barco, sin vosotros hubiera sido mucho más duro.

A l'Alba Valls, per tot el que hem viscut durant aquests 5 anys. Hem estat inseparables des de primer de carrera i espero mantenir aquesta amistat molts anys més, encara que hi pugui haver oceans pel mig. Has estat un gran suport per mi i t'ho agraeixo molt.

Thanks to Shane Kelley for making everything easy.

Gràcies també als meus pares que sempre m'han donat suport i llibertat, motivant-me a tirar endavant i a esforçar-me pel que vull.

Contents

1. Introduction

1.1 The relationship between carbon dioxide and global climate change

Natural variability of the global climate is also affected by human activities. These activities strongly influenced the modern climate change, which are now large enough to exceed the bounds of natural variability. The main source of global climate change is human-induced changes in atmospheric composition (Karl and Trenberth, 2003).

Atmospheric carbon dioxide (CO_2) is a "greenhouse" gas, gas that is transparent for ultraviolet radiation (the one that arrives to Earth from the Sun) but absorbs infrared radiation (radiation emitted from the Earth) causing the surface of the planet to warm. To maintain normal surface temperatures, it is necessary to have a certain concentration of these gases in the atmosphere (Rye *et al.*, 1995). Atmospheric carbon dioxide emissions increased at a rate of 2.8 petagrams of carbon per year (Pg C $year^{-1}$) during 1988 to 1992 (1 Pg = 10^{15} grams). (Fan *et al.*, 1998) The increase of the concentration of this "greenhouse gas" is from 317.66 ppmv in 1961 to 383.57 ppmv in 2007 (Keeling *et al.,* 2008), like various scientific data suggests, might be in fact the cause of increase in temperature (Houghton *et al.*, 1990).

Global analysis shows that the biosphere systems absorb approximately about 60% of anthropogenic fossil fuel emissions, partitioned between absorption by the oceans and storage in terrestrial ecosystems (Quay *et al.*, 1992; Le Quéré *et al., 2007).* These sinks are highly variable and sensitive to climate but they are essential to understand these natural mechanisms of CO_2 uptake that, at the same time, will give us a better comprehension about forecast changes in atmospheric carbon dioxide related with temperature and we will be better able to predict possible changes in the Earth's climate.

1.2 The ocean carbon cycle

The ocean plays a crucial role in the climate system through thermohaline circulation, which transfers warm water from the tropics to the polar regions, and it seems to be sensitive in regards to the rate of change of atmospheric CO_2 concentrations (Stocker and Schmittner, 1997). In addition, oceans are a significant sink for anthropogenic carbon dioxide, taking up about a third of the emissions arising from fossil-fuel use and tropical deforestation (Siegenthaler and Sarmiento, 1993).

The carbon dioxide is permanently exchanged between the atmosphere and water through the process called 'diffusion' to arrive to an equilibrium (Fig. 1). The final equilibrium between the ocean and the atmosphere finds 70-83% of the fossil fuel release sequestered in the ocean that will last for hundreds to thousands of years (Archer *et al.,* 1998). Thus oceans are also the main long-term sink for atmospheric carbon dioxide and play an important role in controlling the rate at which carbon dioxide is increasing in the atmosphere.

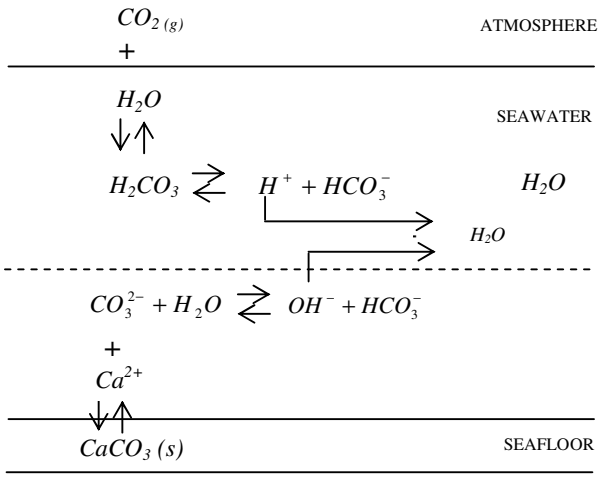

Fig. 1: CO_2 / CO_3^- system. Equilibrium between atmosphere and seawater and between seawater and seafloor.

Approximately 93% of the carbon in the biosphere is located in the ocean (Feely *et al.,* 2001). Phytoplankton converts carbon dioxide and water to carbohydrates and oxygen through photosynthesis and these carbohydrates are then used by all forms of ocean life in order to obtain energy. Thus, the CO_2 fixed in photosynthesis is transferred to the interior of the ocean resulting in a temporary or permanent storage of carbon, keeping it outside of the atmosphere for long periods of time. This process removes carbon from surface waters by gravitational settling, diffusion, and active biotransport of organic carbon and inorganic carbon (namely $CaCO_3$) derived from biological production in the surface ocean and it is known as the 'biological pump'.

A large part of the CO_2 taken up by phytoplankton is recycled near the surface while the rest sinks into the deep waters. This part of photosynthetic carbon that settles in the deeper waters is better known as "marine snow". Marine snow, constituted by phytoplankton, bacteria and detritus, is therefore important for the removal of particulate organic carbon (POC) from the euphotic zone to the sediments or the deep ocean (Plougl *et al.,* 1999). The study of flux of POC could determine the efficiency of the biological pump, which in turn would give us more information about the sequestration of carbon from the atmosphere into the deep ocean and the enrichment of the seafloor.

The Figure 2 shows a schematic illustration of the role of the biologic pump in the oceans: Phytoplankton synthesizes organic matter from dissolved carbon dioxide (CO_2) and nutrients using light as a source of energy. Some of the organic matter that is formed by the phytoplankton settles or is transported below the surface ocean, past a depth of about 100 m where light is sufficient for photosynthesis. Biological processes in the deep ocean consume the organic matter and oxygen, eventually converting it back into dissolved carbon dioxide and nutrients. The loop is closed by transport of these inorganic substances back into the surface ocean (Sarmiento and Gruber, 2004).

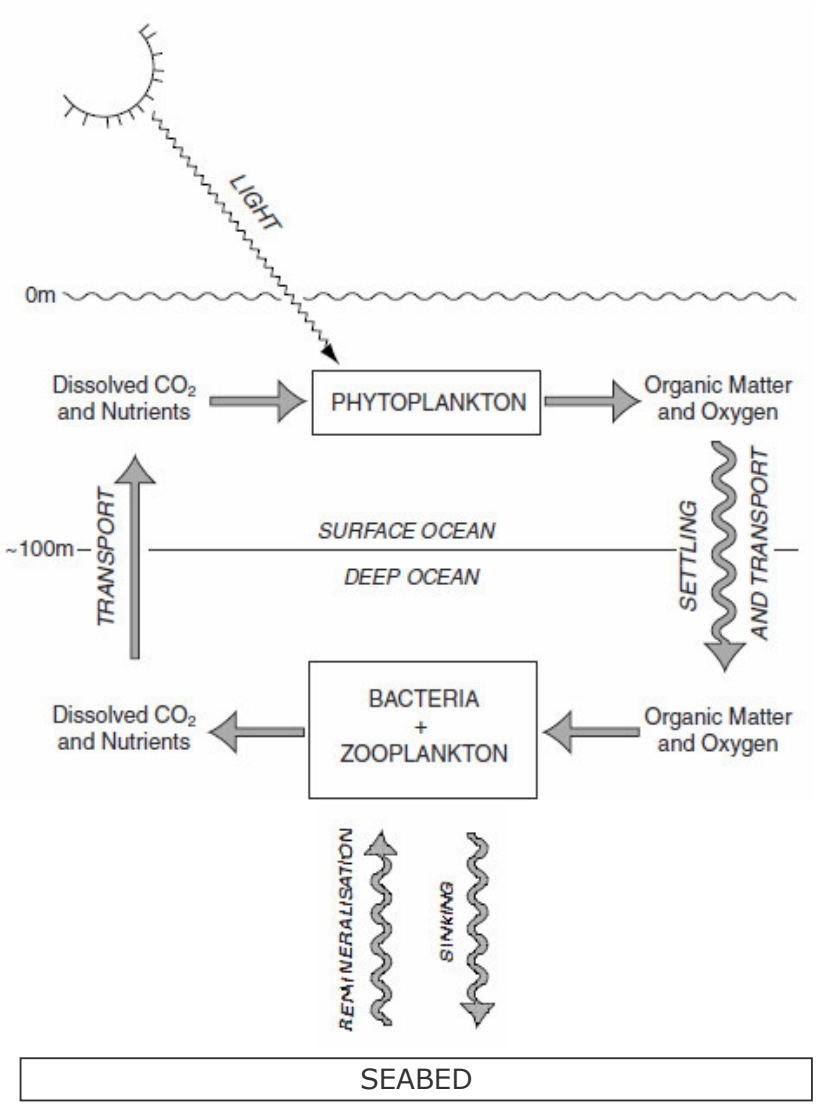

Fig. 2: Simplified diagram of the principal components of the biological pump (Adapted from Sarmiento and Gruber, 2004).

The estimation of the export flux of POC is necessary to understand the global carbon cycle, and it could be done using nutrient balances in the euphotic zone (Ducklow *et al.*, 2001) or geochemical mass balance (Emerson *et al.*, 1997). It can also be used sediment traps, which are the only direct approach for collecting and measuring the vertical particulate flux (Burns and Rosa, 1980; Honjo and Doherty, 1988), or a naturally occurring particle-reactive short-lived radionuclide as a tracer of sinking particles (Cochran *et al.*, 2000; Cochran and Masqué, 2003, Buesseler *et al.,* 2006; Stewart *et al.,* 2006 and 2007; Verdeny *et al.,* 2008), but Buesseler (1991) compared ^{234}Th flux estimates with sediment trap data, and concluded that the radionuclide disequilibrium model (^{238}U-^{234}Th approach) provided a more reliable way of estimating vertical fluxes.

1.3 Disequilibrium of pairs of isotopes to study cycles of particles

The study of particle fluxes using radioactive tracers requires that the radioisotopes used as tracers have specific characteristics, such as an affinity for particles, or particle reactivity, so that they can track the progress of the particles along the water column. Besides, the half-life of the radionuclide is an important parameter if we are interested in quantifying the particle export fluxes. Indeed, the radionuclides are produced and decay at known rates, and so can be used as 'biological' clocks, and can integrate changes in the water column over different time scales depending on the tracer used, ranging from days (^{90}Y, $T_{1/2}$ = 64.3 h), to weeks (^{234}Th, $T_{1/2}$ = 24.1 d), to months (^{210}Po, $T_{1/2}$ = 138.4 d).

Good indirect estimates of POC export using radioactive tracers have been done studying the disequilibrium within the natural radioactive decay series and the ratios between carbon and the radionuclide, like ^{234}Th. In principle, radioactive isotope should be in secular equilibrium with its progeny but, if the parent is soluble and its decay products are particle-reactive, then they can be removed by uptake on particles and the reactive daughter nuclide will be deficient in seawater, relative to the concentration it would have in radioactive equilibrium with its parent. In these cases the equilibrium does not occur, which indicate exportation to deep water (Livingston, 2004). The process can be described and quantified by reservoir models of varying complexity. One of the simplest is the *two-box model* (Fig. 3), where the total activity of the radionuclide of our interest is divided between two compartments, the dissolved and the particulate phase (for further information see Matsumoto, 1975).

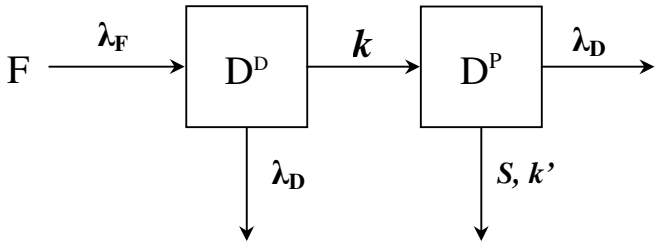

Fig. 3: Schematic diagram of the cycling of a radioisotope in the ocean using a two-box irreversible model. F refers to the father and D to the daughter radionuclides. The figure shows a model of two boxes he first one represents the daughter activity of the dissolved phase and the second one of the particulate phase. λ_F and λ_D are the father and daughter decay constants, respectively, k is the first order scavenging rate constant for uptake of dissolved daughter onto particle surfaces, S accounts for the removal of particles from water column and k' is the removal constant rate, accounting for removal of daughter onto sinking particles. (Adapted from Cochran and Masqué, 2003)

Particle reactive nuclides with relatively short half-lives have been used as tools to determine the export rate of particles from the euphotic zone to the deep ocean. Particle settling velocity has been obtained directly from measurements of the ^{238}U-^{234}Th and ^{210}Pb-^{210}Po disequilibrium in salt water (Santschi *et al.,* 1979; Kershaw *et al.*, 1988). ^{234}Th ($T_{1/2}$ = 24.1 d) and ^{210}Po ($T_{1/2}$ = 138.4 d) are produced by *in situ* decay from their longer lived soluble parent, as it is the case of ^{238}U ($T_{1/2}$ = 4.5·10^9 y). ^{210}Pb ($T_{1/2}$ = 22.3 y), however, is particle reactive, but differs from ^{210}Po, which also becomes incorporated into the cells. Thus, ^{210}Po is more efficiently removed from surface waters than ^{210}Pb (Bacon *et al.* 1988) In addition, their short half-life makes them sensitive to seasonal changes in the processes of POC production and export (Cochran and Masqué, 2003).

Recent studies like Stewart *et al.* (2007) and Verdeny *et al.* (2008) combine the use of these two tracers to study the POC export. The water column profiles of ^{234}Th or ^{210}Po provide information on the processes that occurred previous to the sampling time. Depending on the half-life of the radionuclide that one using the processes are integrated over different time scales, of days to weeks for ^{234}Th, and months for ^{210}Po. Therefore the combined use of these two tracers gives a complementary and more robust approach to study the particle settling along the water column (Cochran and Masqué, 2003).

1.3.1 POC flux estimates derived from radioisotopes

Buesseler *et al.* (1992) proposed an approach using the deficiency in total ^{234}Th with respect to ^{238}U. This difference indicates a flux of ^{234}Th associated with particles sinking out of the euphotic zone, and if the POC/^{234}Th of these sinking particles is known, a POC flux can be calculated as follows:

$$\mathrm{POC}_{\mathrm{flux}} = \mathrm{P}_{\mathrm{Th}} \times \frac{\mathrm{POC}}{^{234}\mathrm{Th}} \qquad (1)$$

where P_{Th} is the flux of ^{234}Th

The formula need to quantify P_{Th} it is necessary to integrate ^{234}Th deficit as (Equation 2):

$$P_{Th} = [\lambda_{Th} \int (A_U - A_{Th}) dz] \qquad (2)$$

As it is shown in Equation 1, the POC/^{234}Th ratio on sinking particles has to be estimated hence, it is necessary to take particle samples from sediment traps or from the *in situ* pumps besides the water samples. Doing this approach it is assumed that sinking biogenic particles are the most important carriers of ^{234}Th. The POC/^{234}Th ratio is usually obtained from particles collected below the photic zone, considering them as representative of those being exported at depth.

In a similar way it is possible estimate the POC flux with other pairs, like ^{210}Po-^{210}Pb (see Verdeny *et al.* 2008) or ^{90}Y-^{90}Sr.

1.4 ^{90}Sr-^{90}Y disequilibrium

Strontium-90 (^{90}Sr) is a radioactive isotope of strontium, with a half-life of 29.1 years. When it decays emits a beta particle, the average decay energy is 0.2 MeV and maximum decay energy of 0.5 MeV. Its daughter, yttrium-90 (^{90}Y) ($T_{1/2}$ =64.3h), is also a beta-emitter with decay energy of 0.9 MeV of average decay energy and 2.3 MeV of maxim decay energy. ^{90}Y decays in ^{90}Zr, a stable isotope. The decay diagram is showed in Fig. 4.

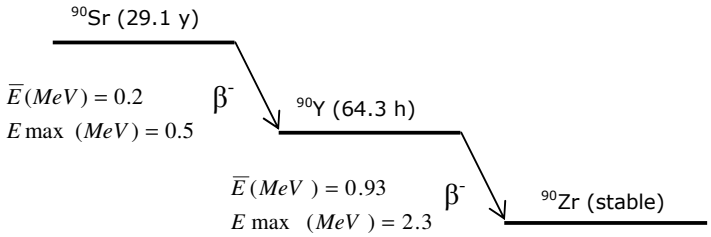

Fig. 4: ^{90}Sr decay chain. Type of emission, half-life, average decay energy and maximum decay energy of ^{90}Sr and its daughter (Choppin, 2001)

1.4.1 Sources of ^{90}Sr

^{90}Sr is one of the main anthropogenic radionuclides of environmental significance, together with the ^{137}Cs and ^{239,240}Pu, produced from nuclear fission of uranium and plutonium in nuclear reactors and in nuclear weapons. For that reason is present in significant amount in spent nuclear fuel and in radioactive waste from nuclear reactors and in nuclear fallout from atmospheric nuclear weapons tests.

The main contribution to the global manmade-radiation environment has come from the testing of nuclear weapons in the atmosphere (Livingston, 2004). The accident at the Chernobyl nuclear power plant (April, 1986) also introduced a large amount of this radionuclide in the environment but ^{90}Sr is found in the environment principally for the widely dispersion that it had from the 1950s until 1980 from the atmospheric testing of nuclear weapons.

The first atomic bomb (called Trinity) was detonated by the United States in July 1945 in New Mexico. This was the first atmospheric nuclear explosion of a total of 520 atmospheric nuclear explosions (including 8 underwater) that took place between 1945 until 1980 (UNSCEAR, 1993).

The periods of intensive testing were in the years 1952-1954, 1957-1958 and 1961-1962 (UNSCEAR, 1993). In 1963 the Union of Soviet Socialist Republics, the United States and the United Kingdom of Great Britain and Northern Ireland agreed to an atmospheric test-ban treaty (Treaty Banning Nuclear Weapon Tests in the Atmosphere, in Outer Space and Under the Water) according of the United Nations which would try to reduce or suppress the production and testing of all kinds of weapons, including nuclear weapons, and in order to put an end to the contamination of environment by radioactive substances.

The amount of ^{90}Sr produced in all atmospheric nuclear tests to 1980 is around 733 PBq and about 1.4 PBq of the ^{90}Sr deposit was associated with Chernobyl accident. All this strontium has been slowly decaying since then so, by 2000, the ^{90}Sr deposit was about 245 PBq (Livingston, 2004).

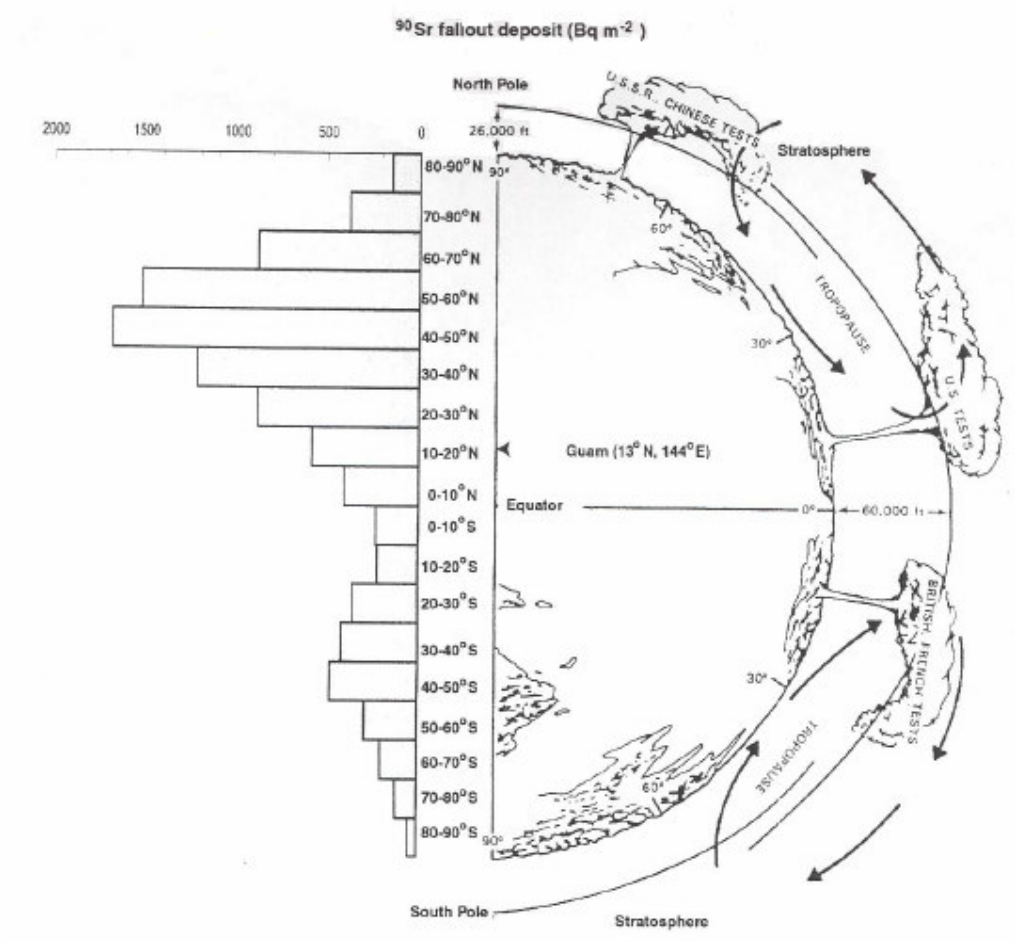

Fig. 5: Schematic diagram of transfer mechanisms between atmospheric compartments (to right) and the measured latitudinal fallout deposit of ^{90}Sr (through 1990, to left) (Hamilton, 2001).

As is showed in Figure 5, the distribution of fallout is not the same in the two hemispheres. These differences are basically due to the locations of the test sites. Between the hemispheres the atmospheric exchange in the stratospheric layer is not too high and the majority of the atmospheric nuclear weapons tests have been done on the Northern hemisphere, for that reasons the amount of fallout in this hemisphere is remarkably bigger.

1.4.2 ^{90}Sr in the oceans

About 70.8% of the Earth surface is covered by oceans, therefore constituting the largest pool of the anthropogenic radionuclides. The inputs of these radionuclides can be directly from the atmospheric deposition, indirectly through the rivers or discharged in the oceans as liquid or solid waste.

Different measurements of radionuclides in the oceans demonstrated that global fallout from atmospheric nuclear weapons tests penetrated into the deep ocean but more studies are required in order to obtain a consensus about the significance of ^{90}Sr penetration into the deep ocean or on the total oceanic inventory (Livingston, 2004).

Other important sources of artificial radioactivity in the marine environment include the dumping of nuclear waste from research, medical or industrial activities, controlled effluent discharges associated with nuclear fuel cycle and nuclear weapons production activities, accidents and/or losses at sea involving nuclear materials, but the amount released by this kind of sources are not always clear because lack information.

The observed activity concentration of ^{90}Sr in surface waters of the Southern hemisphere is much lower than those measured for northern latitudes. Regional anomalies are also identified in association with discharges from reprocessing plants, upwelling and other oceanographic processes (Livingston, 2004).

The total input from all sources of ^{90}Sr to the world ocean has been 383 PBq (377 PBq from global fallout, that includes the inventory on land removed by runoff (~9%), and 6.5 PBq from reprocessing) (IAEA, 2005).

The inputs of ^{90}Sr into the oceans from global fallout are synthesized in Table 1.

Table 1: Summary of ^{90}Sr input to the world ocean from global fallout (PBq)

Latitude	Arctic Ocean	Atlantic Ocean	Indian Ocean	Pacific Ocean	Total	Ocean area 10^{12} m^2
N 90°-60°	4.6	10.2	0.0	1.3	16.1	17.2
N 60°-30°	0.0	57.3	0.0	71.6	128.9	46.8
N 30°-0°	0.0	30.8	13.3	65.8	109.9	90.6
S 0°-30°	0.0	10.3	14.6	26.6	51.5	98.0
S 30°-60°	0.0	15.4	22.5	25.8	63.7	88.2
S 60°-90°	0.0	1.7	2.1	3	6.8	20.4
Total	**4.6**	**125.7**	**52.5**	**194.1**	**376.9**	**361.1**

Data source: IAEA, 2005

For the study of the distribution of radionuclides in seawater the International Atomic Energy Agency (IAEA) made a report of a coordinated research project. The Figures 6 and 7, represent the oceans and seas divided according to their latitude on the basis of known ocean current systems, the location of nuclear test sites, the availability of recent data and, the probability of a relatively uniform distribution of some radionuclides. The Table 2 shows the activity concentration of ^{90}Sr in surface waters of the world's oceans and seas and the geographical zone of the data is indicated with name of the water mass and with its corresponding latitudinal box number shown in Figures 6 and 7.

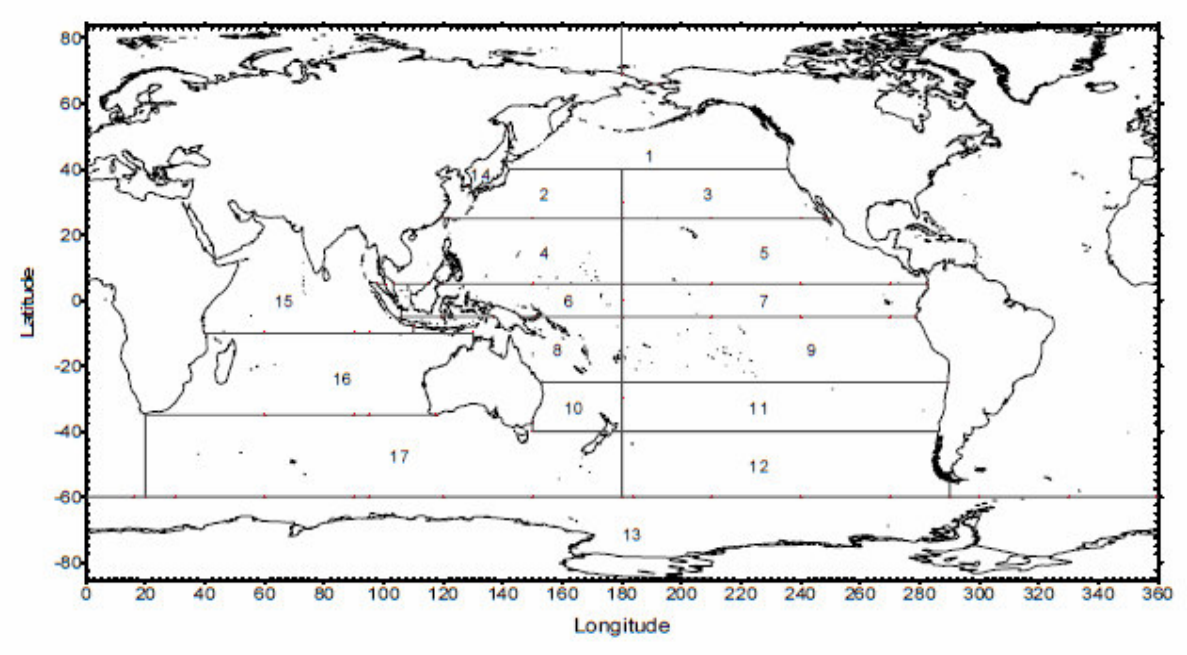

Fig. 6: Latitudinal boxes in the Pacific and Indian Oceans (IAEA, 2005)

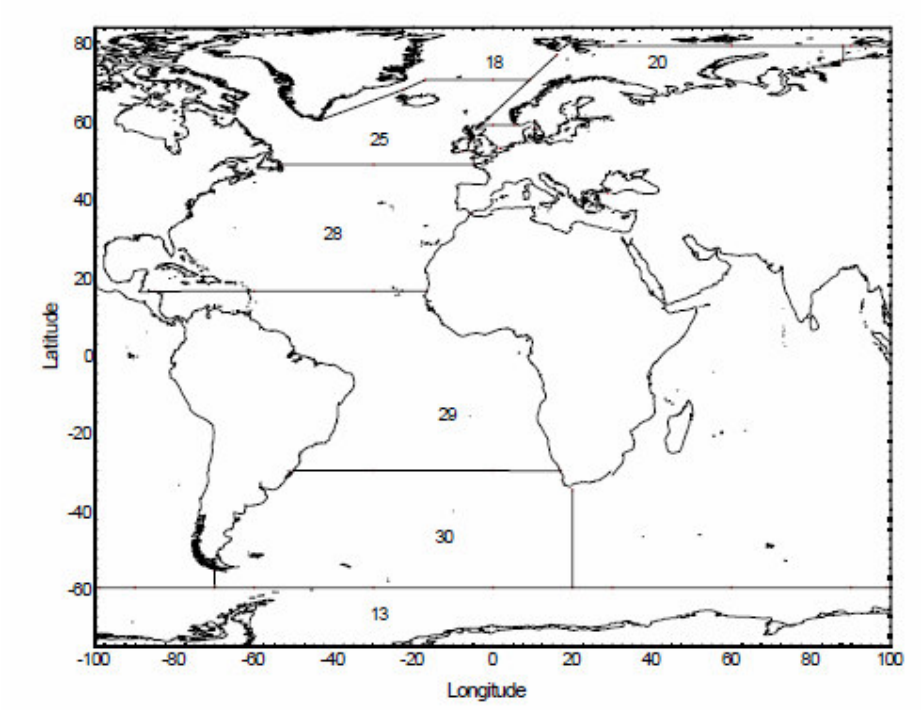

Fig. 7: Latitudinal boxes in the Atlantic Ocean (IAEA, 2005)

Table 2: ^{90}Sr in surface water of the world's oceans and seas

Area	Box No.	Number of data	Averaged value on 01.01.2000 (mBq/L)	
			Box	Area ± 1σ
North Pacific	1	3	1.3	1.4 ± 0.2
	2	31	1.6	
	3	3	1.4	
	4	13	1.5	
	5	5	1.1	
Equatorial Pacific	6	2	1.5	1.3 ± 0.3
	7	3	1.1	
South Pacific	8	1	1.2	0.8 ± 0.3
	9	4	1.1	
	10	3	0.8	
	11	4	0.6	
	12	2	0.4	
Antarctic	13	1	0.1	0.1
Sea of Japan	14	42	1.6	1.6 ± *0.3*
Arabian Sea	15	15	1.0	1.0 ± *0.2*
Indian Ocean	16	7	1.1	1.1 ± *0.2*
Southern Ocean	17	12	0.7	0.7 ± *0.4*
Arctic	18	1	2.3	2.3
	19			
Barents Sea	20	7	1.9	1.9 ± *0.4*
Baltic Sea	21	71	11.1	11.1 ± *2.9*
North Sea	22	118	4.0	4.0 ± *1.2*
Irish Sea	23	14	49	49 ± *83*
English Channel	24	43	4.1	4.1 ± *1.4*
North N. Atlantic	25	17	2.1	2.1 ± *0.9*
Black Sea	26	15	17	17 ± *6*
Mediterranean Sea	27	15	1.7	1.7 ± *0.2*
North Atlantic	28	17	1.2	1.2 ± *0.6*
Central Atlantic	29	5	0.8	0.8 ± *0.1*
South Atlantic	30	2	0.4	0.4 ± *0.2*

Normal Font: Standard deviation for area-averaged value
Italic Font: Standard deviation for box-averaged value

Data source: IAEA, 2005

The most appropriate places to carry out future work using the method of ^{90}Y/^{90}Sr to study the particle cycling are seas with a high activity concentration of ^{90}Sr like the Baltic Sea, the Black Sea or the Irish Sea (see Table 2). Also, they are shallow seas, overall the Baltic Sea and the Irish Sea, with low rates of water renovation, hence they have a high particle concentration, with a range between 5mg/L and 55mg/L, (Kriztsov *et al., 2008;* Siegel *et al.* 2009) so, probably making it easier to observe disequilibrium between both radionuclides.

Collected samples for this project have been taken from the Mediterranean Sea, due to proximity, and the Pacific Ocean, because we had the opportunity of participate in a cruise that took place in the Eastern Tropical North Pacific, therefore, the inventories below are focused in these areas.

Mediterranean Sea

The Mediterranean Sea is the biggest interior sea of the world communicated with the Atlantic Ocean through the Strait of Gibraltar. It is a concentration basin which means that the amount of water evaporated is higher than the contributions of precipitation and runoff. That negative balance makes that the salinity of the sea increase (37.5 g/L) and it becomes superior to that of the Atlantic Ocean (36-36.5 g/L) (IAEA, 2005). This characteristic must be taken in consideration to understand the water circulation of the sea.

Artificial radionuclide concentrations and inventories are highly variable in the Mediterranean Sea, highest on the continental shelf and near river mouths and lowest in deep-sea environments (IAEA, 2005), as a consequence of the land inputs carried by the runoff or the controlled effluent discharges.

The major source of anthropogenic radionuclides to the Mediterranean Sea is fallout from atmospheric weapons testing in the early sixties but, due to the proximity of the nuclear power station of Chernobyl the fallout released from its accident was significant, but nowadays, as is presented in the Table 3, ^{90}Sr has decayed and the inventory due to the Chernobyl accident is, in PBq, negligible.

Table 3: ^{90}Sr inventories in the year 2000 in the Arctic and Atlantic Oceans (PBq)

Latitude	Global fallout	Local fallout	Repro-cessing	Chernobyl	Subtotal
^{90}Sr					
N 90°-30°	28.8	0.0	3.9	0.0	32.7
N 30°-0°	12.3	0.0	0.0	0.0	12.3
S 0°-30°	4.1	0.0	0.0	0.0	4.1
S 30°-90°	6.8	0.0	0.0	0.0	6.8
TOTAL	52.1	0.0	3.9	0.0	56.0

Data source: IAEA, 2005

The mean activity concentration of ^{90}Sr in the Mediterranean if of 1.7±0.2 Bq/m^3 (decay corrected for 2000) (IAEA, 2005).

Pacific Ocean

The Pacific Ocean is the largest of the Earth's oceanic divisions. It represents about 46% of the Earth's water surface. The latitudinal variation is so large that the rank of temperature, salinity, and other water characteristics is very wide.

The major source of anthropogenic radionuclides in the Pacific Ocean and its marginal seas can be traced to global and local fallout from nuclear weapons testing. The total amount of ^{90}Sr from global fallout is 605 PBq and about 113 PBq are inputs from local fallout due to the United States Pacific tests (IAEA, 2005)**.** The amounts of radionuclides introduced by other sources are smaller.

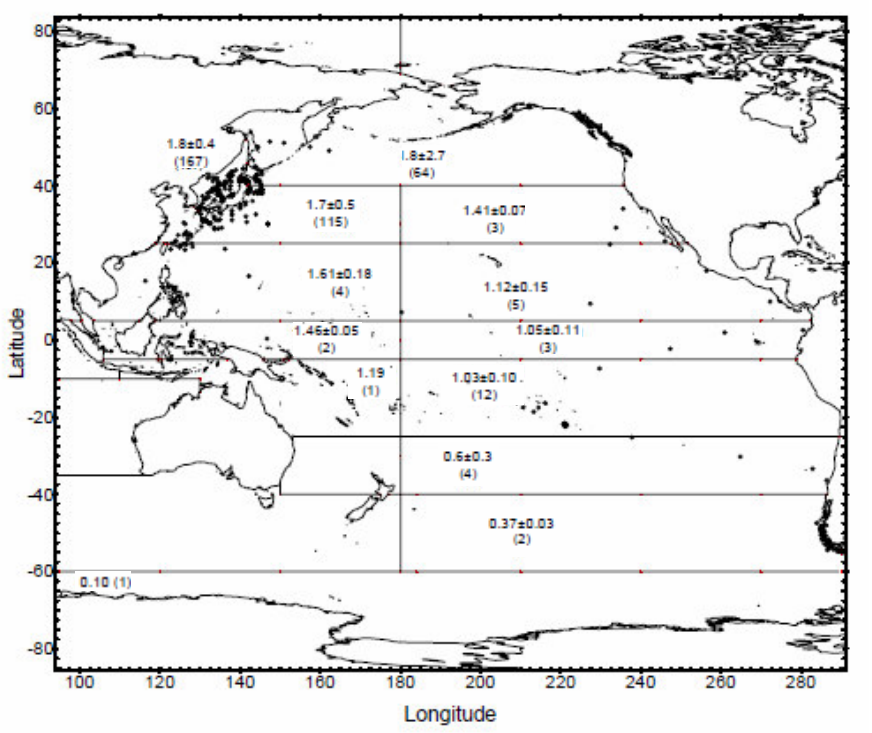

Fig. 8: ^{90}Sr in surface water (1991-1995), decay-corrected to 01-01-2000, in mBq/L (IAEA, 2005)

The activity concentrations of ^{90}Sr show a relationship with latitude: the highest values of its specific activity (1.8 mBq/L) are found in the North West of the Pacific Ocean (Fig. 8), and the lowest concentrations reported by IAEA (2005) are found near to the Southern Ocean (0.4 mBq/L).

1.4.3 ^{90}Sr-^{90}Y disequilibrium to estimate the POC export

Strontium is a quasi conservative element in seawater, thus its distribution in the oceans is determined by physical processes like mixing and diffusion. Strontium and calcium have similar behaviors and both can be accumulated by organisms. The mechanism of accumulation could be the precipitation as insoluble inorganic structures (in mollusks and corals) or retained in the ion-exchange system (as in sea weeds) (Bowen, 1956). The microorganisms also assimilate these elements, and Sr could substitute Ca from $CaCO_3$ in order to form $SrCO_3$, but the fraction of Sr that substitute Ca is small (2%-3%) (De Villiers, 1999).

Yttrium is a particle-reactive element, and thus it has a more rapid removal from the surfaces due to its affinity for particles, and is removed with them as particles settle to deep waters. This enables to use this pair of radionuclides to study the POC export from the upper ocean. The short half-life of ^{90}Y, of only 64.3 h, implies that it could be used to estimate daily timescales of this export.

Orlandini *et al.* (2003) proved this proxy in freshwaters from the Savannah river where concentrations of ^{90}Sr are large enough to carry out studies of particle dynamics employing the ^{90}Sr-^{90}Y disequilibrium.

In this work we expand the measurement of radiogenic disequilibrium to a seawater system under the hypothesis that the disequilibrium between ^{90}Sr and its daughter ^{90}Y can be used to gather information about the export fluxes of POC in the oceans. We shall eventually compare this data with the information obtained from other short-lived radionuclides like ^{234}Th ($T_{1/2}$ = 24.1 d) and ^{210}Po ($T_{1/2}$ = 138.4 d), that are appropriate for a larger time scale.

In order to be able to carry out this final objective, first it is necessary to test a method to separate ^{90}Y from its father, ^{90}Sr.

2. Materials and methods

The quantification of the disequilibrium between ^{90}Sr and its daughter (^{90}Y) requires that they are concentrated and isolated from the sample.

Low activities make necessary to use large volume sample (of about 50-100 L). The minimum detectable activity (MDA) had been calculated in order to know the sea water volume that must be collected to ensure that we will be able to measure the activities of ^{90}Sr and ^{90}Y with enough precision. The MDA for the beta counter used in this work (see below) is 8.3 mBq, while the average activity of ^{90}Sr in seawater is 1.4 mBq/L (calculated using the data from IAEA (2005) decay-corrected to 01-01-2009). Sampling 10 L of water the sample will have an activity of the same order of the MDA but this is the worst situation because if we have losses during the procedure the activity will be below this limit, for that reason is important to collect ~100 L of seawater in order to be above the MDA at least by an order of magnitude.

These samples need to be concentrated to obtain detectable concentrations in small volumes. Moreover, ^{90}Y is a beta emitter, and therefore radiochemical analysis and purification of the samples to eliminate the interference of other beta emitters as ^{234}Th, must be carried out to ensure that the measured activity comes only from ^{90}Y.

The radiochemical protocol is shown in Figure 9, and was developed by adapting the method used by Orlandini *et al.* (2003).

Separation of ^{90}Y from the sample: First co-precipitation

Concentrated hydrochloric acid (HCl, PA grade) (~80 mL) is added and well stirred, and then wait a few minutes before adding 2 mL of Y^{+2} carrier (1 mg/mL) and 2 mL of Fe^{+3} (30 mg/mL)[1]. The sample is gently stirred for a few minutes, and then allowed to equilibrate for an hour.

After 30 minutes the sample is neutralized with NH_4OH or NH_3 to pH 8.5. It will then form a precipitate of iron hydroxide, $Fe(OH)_3$, and ^{90}Y will co-precipitate. The precipitate is left to settle from 1-2 hours before filtering.

Filtration and dissolution of the iron-precipitate

The iron precipitate is filtrated through GF/F filters (Schleicher & Schüll) 142mm, 8µm of porous diameter, using a peristaltic pump. The filtered sample is stored for 15 days, the time necessary to have ^{90}Sr and ^{90}Y in equilibrium for a later measurement of ^{90}Y to get the activity concentration of its father.

The iron hydroxide from the filter must be dissolved with 20mL 8M HNO_3. Aliquots are taken to assess losses through the process by measuring stable Y by *Inductive Coupled Plasma Optic Emission Spectrometry* (ICP-OES).

[1] 145.2g $FeCl_3 \cdot 6H_2O$ up to 1L in deionized water

Purification: Ion-exchange columns

Anion column AG 1-X8

The 20mL of sample are transferred to an anion column consisting of 3.5mL BIORAD AG1-X8 resin (100-200 mesh). The column has been pre-conditioned with 10mL of 8M HNO_3. This column retains thorium, and yttrium is elutes in 8M HNO_3. To ensure that all the yttrium is eluted, the column is washed with additional ~20mL 8M HNO_3 (in four rinses). The eluted solution (yttrium fraction in 8M HNO_3) is collected in a Teflon beaker and heated to state of dryness.

Cation column AG 50W-X8

The yttrium fraction is dissolved in 20mL of 1M HCl and transferred to a cation column of 3mL BIORAD AG 50W-X8 (100-200 mesh) resin, preconditioned with 10mL of 1M HCl. The resin retains the yttrium while Sr, Fe, or Ca are eluted. Then, the column is washed with 80 mL 1M HCl in various rinses. Yttrium is eluted adding 30mL of 6M HCl in three rinses. This fraction is saved and an aliquot is collected to determine the chemical recovery.

Recovering the ^{90}Y. Last co-precipitation

Next, 1.8mg of Fe^{+3} is added to the Y fraction, and NH_4OH or NH_3 to raise the pH to 8.5 and makes $Fe(OH)_3$. The precipitate was filtered through a 25 mm diameter Whatman (cellulose nitrate) 0.45µm.

Finally, the filter is dried and placed on a beta holder, covered with a plastic foil for a beta counting using a gas-flow proportional beta counter.

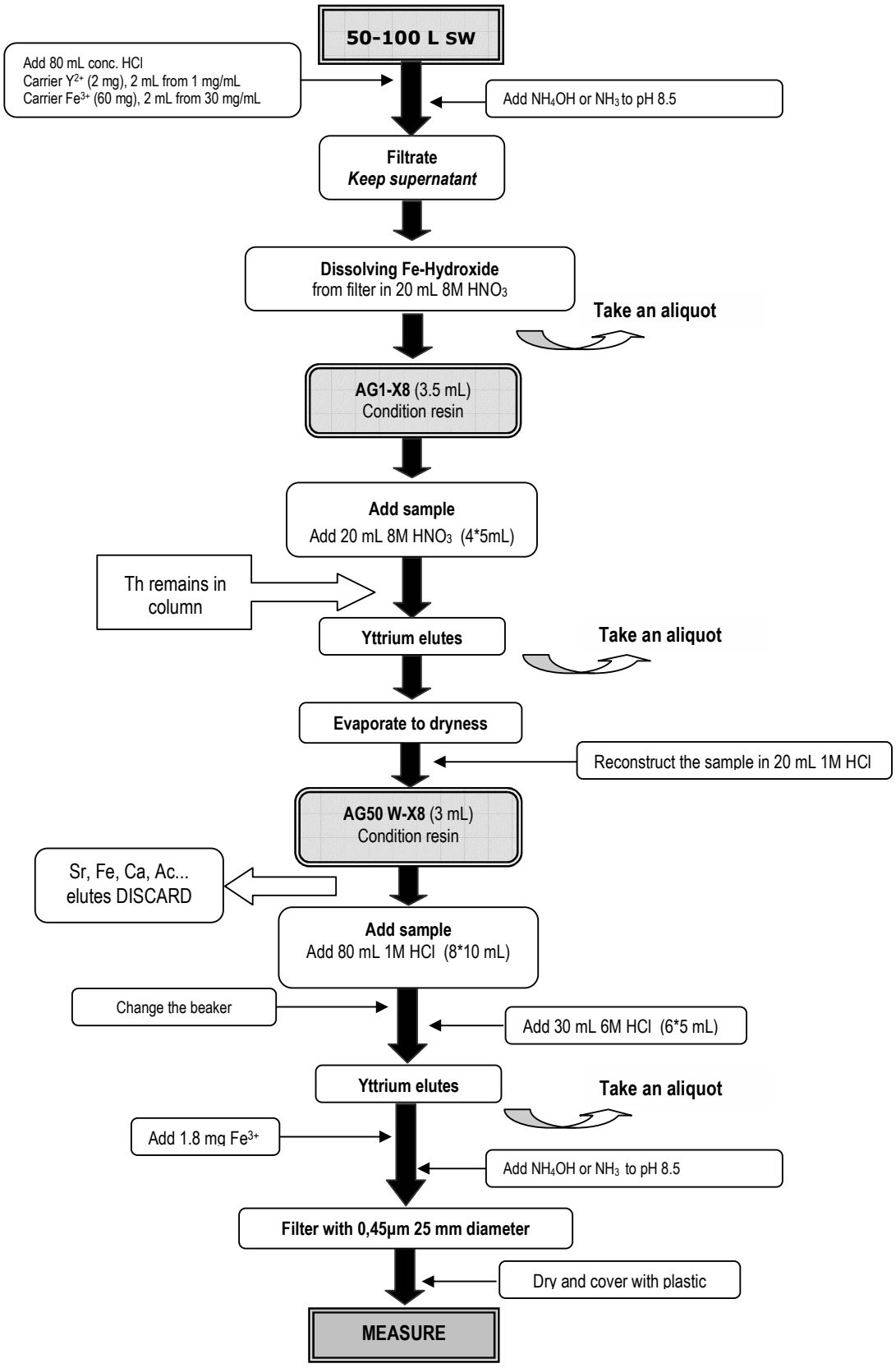

Fig. 9: Radiochemical protocol to purify yttrium from seawater samples.

2.1 Testing the method (I): Mediterranean samples

To test this procedure, several samples of 50 L of pre-filtered surface seawater were collected from the Aquarium of Barcelona.

The procedure employed to do this samples was different from the former, which has been explained above because at the beginning we have used different quantities of reactive, tracers or resins in order to test and improve the procedure.

After some tests, we proved that the volume of hydrochloric acid used to acidify the sample could be reduced from 500mL to 80mL. The volume of iron added at the end for the last precipitation of the yttrium has been tested too, and it has been reduced from 500µl to 60µl. The amount of iron added was therefore a compromise between being sufficient to scavenge the yttrium and small enough to obtain a reproducible geometry for determination in the beta counter. This last constrain is based on the fact that if the iron precipitate forms a thick layer when filtered, the beta emission are self-absorbed before they can be detected.

Fifteen days later the procedure was repeated with the filtrated water that we had saved from the first filtration to calculate the activity of ^{90}Sr by means of the measurement of ^{90}Y produced by ingrowth from ^{90}Sr.

With these tests we proved the method in order to be able to isolate and measure the yttrium with good recoveries, and we also improved the initial method thinking in the future applications.

2.2 Testing the method (II): GoCAL4 cruise, oceanographic campaign in the Gulf of California

The GoCAL4 cruise took place from the 10th of July to the 8th of August of 2008, within the framework of the project "*Nitrogen Fixation and its Coupling with Denitrification in the Eastern Tropical North Pacific (GoCal)*" (National Science Foundation, USA), co-leaded by Fred Prahl, Brian Popp and Claudia Benitez-Nelson. The main objective of this project was to study the organisms that fix atmospheric nitrogen gas (N_2) converting it into bioavailable forms (NH^{+4}, NO^{3-} and NO^{-2}) and its consequences into the particulate flux in this area. These organisms can increase the primary production and the exported carbon flux, and one of the main objectives of the project is to better understand the processes that regulate the capacity of the oceans to absorb CO_2.

Our contribution to this project consisted on using the natural radionuclides $^{234}Th/^{238}U$ and $^{210}Po/^{210}Pb$ to study the export fluxes and remineralization of organic carbon and nitrogen along the water column. This was a very suitable opportunity to test the $^{90}Y/^{90}Sr$ method that we had been developing in the laboratory.

2.2.1 Study area

The GoCAL4 cruise was carried out in the Gulf of California (also known as the Mar de Cortés) and the adjacent waters of the eastern tropical North Pacific (Fig.10). The Gulf of California is a mass of water that separates the Baja California Peninsula from the Mexican mainland. It is unique because this area has been detected as one of the highest in primary productivity in the world oceans (Bustos-Serrano, 2006).

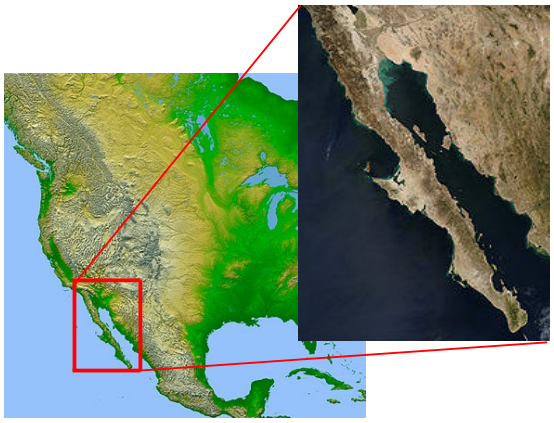

Fig.10: Gulf of California

The main objective of this cruise was to study the nitrogen fixation and its coupling with denitrification and this area was interesting for its rich biological productivity and also, because these waters are subjected to the inflow of denitrified (N poor) waters from the subtropical Pacific during the summer, when thermally stratified waters promote high rates of N_2 fixation (Benitez-Nelson, Annual Report, 2008).

During the GoCAL4 cruise 7 stations were occupied (Fig. 11). The samples to study the disequilibrium between ^{90}Sr and ^{90}Y were collected of the 20.5ºN 106.5ºW.

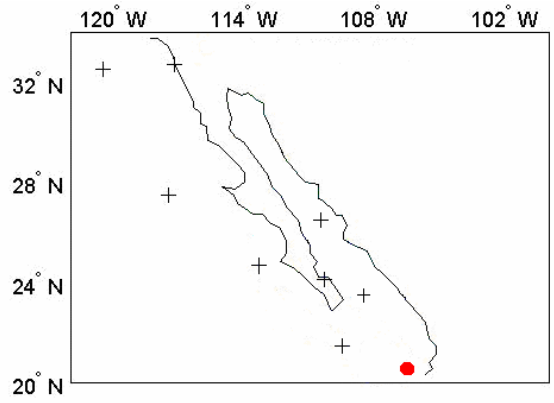

Fig. 11: Study area with the 7 stations. The circle corresponds to the station where water to study $^{90}Y/^{90}Sr$ disequilibrium was sampled.

2.2.2 Sampling

To obtain the water samples we used a CTD rossette equipped with 24 Niskin bottles (Fig. 12). The CTD is a sensor which provides information on chlorophyll a, temperature and density, as well as salinity and transmissivity. This equipment is deployed to the sea and descends to a depth of approximately 1000m), picking up data from the water column, which gives the results in the computer.

Fig. 12: CTD rossette equipped with 24 Niskin bottles.

Having the profile of the different characteristics from the water column, we chose the depths where we wanted to pick up samples. The equipment must be programmed in this manner, as it is going up, the Niskin bottles, of ~10L each, are closed at the particular depths and collect the water.

Fig. 13: Sampling barrel

To study the $^{90}Sr/^{90}Y$ disequilibrium it was necessary to use large volumes of sample (50-100L). For that reason we decided to divide the 24 Niskin bottles into three groups, 8 bottles per group. Each group was used to sample water from one depth (Fig. 13; Table 4). Thus, to obtain a profile of 6 depths, it was necessary to cast the CTD rosette with the Niskin bottles twice. The depths for each sample are shown in Table 4.

Table 4: Sampling data

ID sample	Cast	# Bottles	Depth (m)
Y1	1	1-8	130
Y2	1	9-16	100
Y3	1	17-24	70
Y4	2	1-8	40
Y5	2	9-16	20
Y6	2	17-24	5

Fig. 14: Filtering the iron precipitate

The water samples for our study were collected and processed (Fig. 14) using the iron co-precipitation method, further explained in the Materials and Methods section, and they were directly counted using a gas-flow proportional beta counter. After 15 days we repeated the procedure to estimate the quantity of strontium in the samples.

At the radiochemistry laboratory of the Grup de Física de les Radiacions (LRA) of the Universitat Autònoma de Barcelona (UAB) we continued counting the samples to be sure that we only detect counts of the background (all the ^{90}Y must be decayed). The aliquots collected along the procedure were analyzed in the Servei d'Anàlisi Química (SAQ) of the UAB, using ICP-OES, to know the chemical recovery.

2.3 Beta counting and decay corrections

Counting the beta emission has to be done instead of measurement by mass spectrometry because atom abundances of ^{90}Y is not sufficient to permit this kind of measurement.

The beta counter detects charged particles that arrive at the gas and ionize it generating a pulse. All the betas emitted from the samples can be a possible pulse because the beta counting does not discriminate beta measurements. This point has to be considered in order to evaluate the activity of a sample and also, the possible biases induced from the self-absorption (Rutgers van der Loeff *et al.*, 2006).

After the co-precipitation with $Fe(OH)_3$ and the subsequent purification steps via ion exchange columns, all of the beta activity in the sample must be derived from ^{90}Y decay but, as beta counting is not isotopic specific, the possible contribution of other beta emitters (like ^{234}Th) must be considered. For that reason, it is important that samples are counted repeatedly at regular intervals in order to confirm that decay rates of ^{90}Y follows the 64h half-life. ^{90}Y has a very short half-life so, the purification process should be done in the minimum time possible and the repeated counting is especially important soon after collection.

The background was obtained measuring samples from the GoCAL4 cruise when all the ^{90}Y had been decayed. The value obtained was 0.31±0.06 cpm. In the sea we used an empty filter to measure it. Due to the timing, it was not possible to obtain a background from samples once ^{90}Y had decayed and strontium samples were not measured on the sea. The strontium samples were measured at UAB, once decayed. After comparing both backgrounds, a slight increase of counts over the background measured at UAB was observed. Considering that, we did a quotient between the background measured in the sea and the ones measured at UAB, then, the background counts measured in the sea were multiplied by this value to make better background corrections.

During the counting process, the ^{90}Y decays. It has a half-life of the same order of measurement, so we have to calculate its activity according to the date of separation from its father as usual but, also, considering the time of measurement. The decay correction that must be done, including the correction for the measurement time and for the elapsed time between $^{90}Y/^{90}Sr$ separation and the beginning of the measurement, is presented below in the equation 3:

$$A = \underbrace{\frac{(N_T - N_B)\cdot Ln2}{T_{1/2Y}\cdot\left(1-e^{\frac{-Ln2\cdot t_m}{T_{1/2Y}}}\right)}}_{\text{Measurement correction}} \cdot \underbrace{e^{\frac{Ln2\cdot t}{T_{1/2Y}}}}_{\text{Decay correction}} \cdot \frac{1}{Yield\cdot\varepsilon\cdot V} \qquad (3)$$

Where:

N_t are the counts of the sample
N_B are the counts of the background
$T_{1/2Y}$ is ^{90}Y half-life
t_m is the time of the measurement
t is the elapsed time between $^{90}Y/^{90}Sr$ separation and the beginning of the measurement
Yield is the chemical recovery
ε is the efficiency of detection
V is the volume of sample.

The detection efficiency of the beta counter obtained for ^{90}Y was checked to be about 50% (*pers. com.* María Villa), similarly to what is obtained for other beta emitters with the same or higher decay energies.

2.4 Chemical recoveries

High chemical recoveries are necessary to be sure that we can detect the activity of yttrium by beta counting and to estimate the losses along the process. With this purpose a spike of stable Y was done in the samples. The volume added of this tracer was 2 mL of solution with a concentration of 1 mg/mL of Y^{+2}.

During the process several aliquots had been taken and they have been measured at the SAQ by ICP-OES. The data obtained from these measurements have been used to calculate the recovery of the ^{90}Y extraction that will be used to calculate the activity of the samples and the uncertainty of the results. The volume of the aliquots depends on the concentration of tracer that we have in the sample, assuming a 50% recovery, in order to collect aliquots that were above the detection limit of the ICP-OES of 1 ppm. Based on laboratory experiments, recovery of ^{90}Y on the GF/F filters was always greater than 90% (*pers. com.* María Villa).

In addition, some filters have been re-dissolved into 8M HNO_3 to recover the stable yttrium and measured it by ICP-OES in order to compare these results with the ones from the aliquots.

3. Results

3.1 Mediterranean samples

In order to confirm that the decay rate follows the half-life of ^{90}Y the samples were counted repeatedly at regular intervals. An example is shown in Figure 15 which represents the cpm's of different samples that have been measured for 16 days, and we can see how the activity decays exponentially during the counting period.

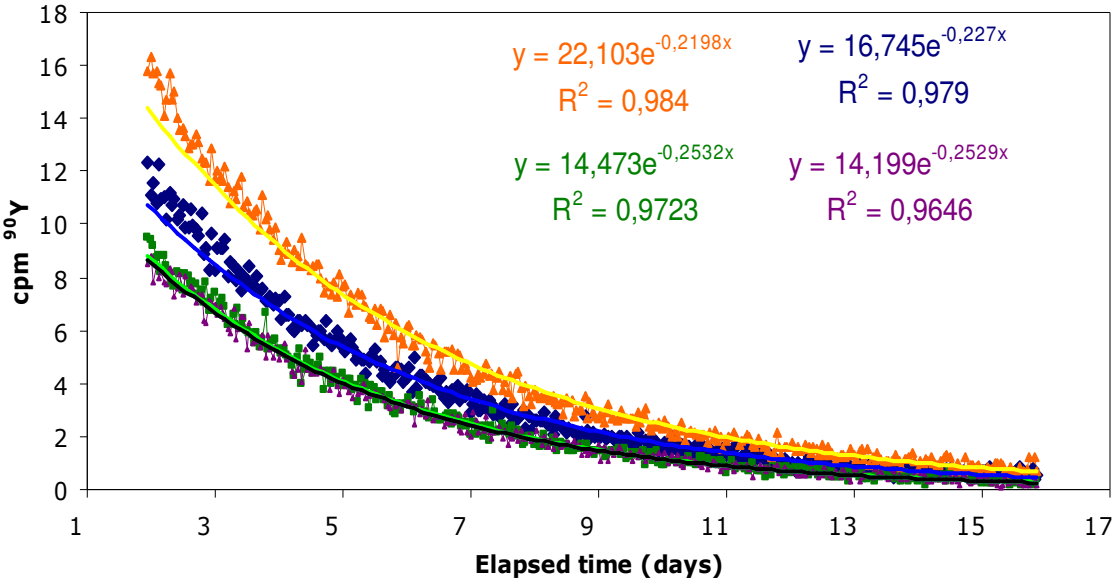

Fig. 15: ^{90}Y exponential decay during the measuring time from several samples

To calculate the decay rate, the data must be corrected considering that ^{90}Y has a half-life of the same order that the elapsed time of the counting, as in equation 4:

$$A = \frac{(N_T - N_b)\cdot Ln2}{T_{1/2Y}\cdot\left(1-e^{\frac{-Ln2\cdot t_m}{T_{1/2Y}}}\right)}\cdot\frac{1}{Yield\cdot\varepsilon\cdot V} \qquad (4)$$

Figure 16 represents the decay during the counting time (t_m = 192 h) of a sample with the corrections done. The half-life obtained indicates that we are effectively measuring ^{90}Y.

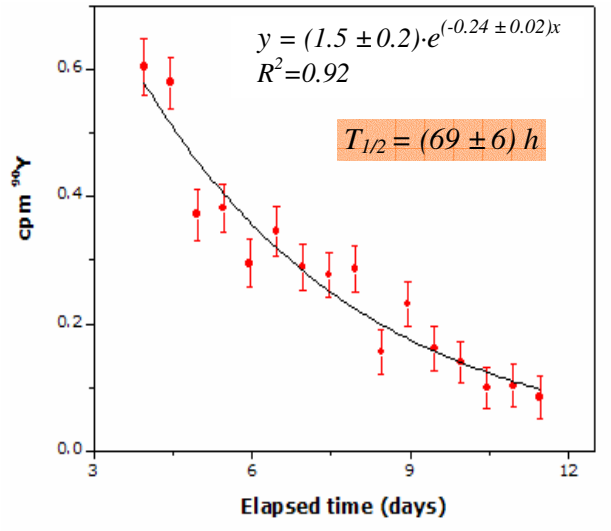

Fig. 16: ^{90}Y decay during the measuring time

3.2 GoCAL4 samples

The data of the ^{90}Sr and ^{90}Y activity profiles collected from the Gulf of California are given in Table 6. The samples were measured in 15 minutes cycles for almost one complete day (see Table 5). In order to calculate the activity of the samples it was necessary to use the equation 3. The sample volume was ~80L and the efficiency of counting was 50%. The chemical recovery was obtained from the aliquot collected after passing the sample through the second column.

Table 5: Information about timing during the procedure

ID	Separation date	Measuring start date	Measuring finish date	Total measuring time
Y1 Y2 Y3	19-7-08 1:15	22-jul-08 4:18	23-jul-08 2:46	22h 27min
Y4 Y5 Y6	20-7-08 15:00	24-jul-08 18:46	25-jul-08 14:55	20h 9 min

Table 6: Activities of ^{90}Y and ^{90}Sr for different depths and recoveries

ID	Depths (m)	^{90}Y A (Bq/m^3)	Recovery	^{90}Sr A (Bq/m^3)	Recovery
Y1	130	1.0 ± 1.5	0.300 ± 0.003	0.2 ± 0.1	0.284 ± 0.003
Y2	100	1.0 ± 1.0	0.294 ± 0.003	0.1 ± 0.1	0.371 ± 0.004
Y3	70	1.0 ± 1.3	0.137 ± 0.001	0.2 ± 0.2	0.354 ± 0.004
Y4	40	1.3 ± 1.2	0.385 ± 0.004	0.1 ± 0.2	0.140 ± 0.001
Y5	20	1.1 ± 0.75	0.418 ± 0.004	0.08 ± 0.1	0.453 ± 0.005
Y6	5	1.0 ± 1.0	0.437 ± 0.004	0.1 ± 0.1	0.449 ± 0.004

4. Discussion

4.1 Procedures

Large sample volumes have to be used due to the low activities of ^{90}Sr in the oceans. This makes the sampling difficult as well as the subsequent procedure of precipitation and separation of ^{90}Y from the water, which takes a long time. In order to reduce the processing time, instead of evaporating the sample after the first column, we make an iron precipitate and we filter it. Then, we only need to dissolve the precipitate with the desired acid and molarity and transfer the sample to the second column.

In relation with timing, another problem often arose when filtering the $Fe(OH)_3$ precipitate from the 80 L initial sample and the filters sometimes were clogged, the flux decreased and then the filter needed to be exchanged, to save time during filtration. Additionally, the working conditions were far from being the best: on a cruise the boat moves, we sometimes needed to work overnight with little light and the wind was usually blowing strongly, so that the processing of the filters was not easy.

Another point that must be considered is the pH for the $Fe(OH)_3$ precipitation. If it exceeds 8.5 then we will obtain a precipitate with a lighter color and it will be very difficult to filtrate. Also, some results suggest that with these precipitates the recoveries are lower. More tests need to be done to estimate the influence of the pH on the final recoveries and on the filtering time.

4.2 Results

4.2.1 Mediterranean samples

Our results proved that ^{90}Y can be isolate from seawater samples using the iron co-precipitation as shown in Figure 16, where the half-life obtained from several samples are in accordance to the theoretical value (^{90}Y, $T_{1/2}$ = 64.3 h).

Another point to emphasize is the recoveries, which have been always greater than 90% (*pers. com.* María Villa).

4.2.2 GoCAL4 samples

4.2.2.1 Counting, Recoveries and Corrections

Counting

During the cruise the time available for measuring was limited, compromised by the amount of samples to be measured and the long measuring times, that ^{90}Y samples shared with ^{234}Th samples that were being collected in parallel and also being measured in the beta counter. Therefore, for ^{90}Y determination the counting was done for ~24 hours, performed in cycles of 15 minutes each in order to maximize the number of cycles. This way we could then group the cycles the most convenient way to obtain more counts and reduce the uncertainty to

determine the activity of the sample. In ideal conditions one would be interested in counting the sample for as long as possible, i.e. over a week, in cycles of 60 min.

Once in the laboratory the tests were done in cycles of 60 minutes because we had more available time. With more minutes of counting for each cycle we obtain higher number of counts which means that the uncertainty is lower and we also can aggregate the data if it is necessary.

Recoveries

The losses during the analytical procedure were assessed by determining the recovery of the process. Stable Y, Y^{2+}, was added at the beginning of the analysis for that purpose, and the measured recovery was associated to be the same as for ^{90}Y, because they are the same element and should behave similarly. Thus, an aliquot was taken at the end of the purification procedure to be measured at SAQ laboratory once back to UAB.

A second determination of the analytical losses was done after all the beta countings necessary to determine the ^{90}Y activity were carried out, i.e. after at least 2-3 weeks when the ^{90}Y had decayed away. Then the filters were dissolved to have all the yttrium in solution and an aliquot was taken and measured by ICP-OES.

The recoveries obtained for the ^{90}Sr (Table 6) have been corrected because it has been calculated that 7% of the stable yttrium added to trace was not retained in the filter and remained in the strontium beaker, which would generate an over-estimation in case of not being corrected.

The results are not too high but considering that was the first time that this experiment was carried out at sea, and knowing the technical difficulties that took place, I think that the results could be valued positively.

4.2.2.2 Profile

In Figure 17 is shown the profile obtained for total activities for ^{90}Sr and ^{90}Y over the upper 130 m of the water column. We can see that it does not show a clear difference between activities of both radionuclides, indicating none disequilibrium between both radionuclides. If these results are compared with the ones obtained by using other POC proxies (^{234}Th and ^{210}Po) we could see that they do not estimate a high export flux of particles. Effectively, POC export fluxes from the upper 150 m obtained using both drifting sediment traps and $^{234}Th/^{238}U$ disequilibrium estimate a flux of 1 to 2 mmol POC m^{-2} d^{-1}. These low fluxes are consistent with the observed little to no deficit of ^{90}Y relative to in the upper waters.

.

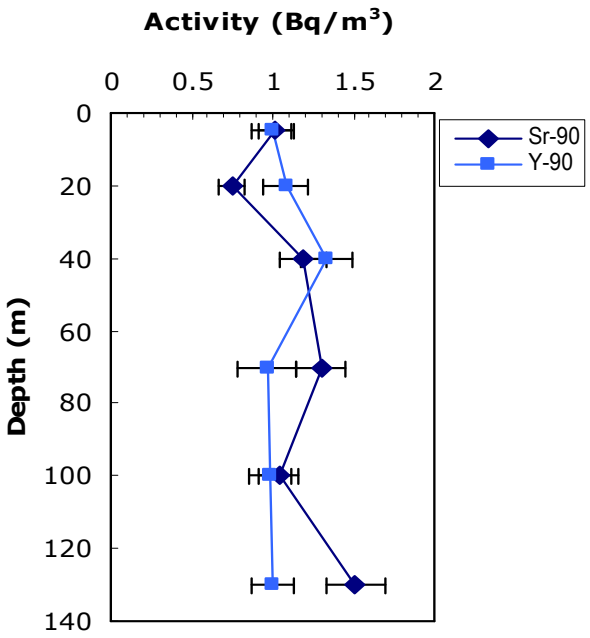

Fig. 17: Activity profile for ^{90}Sr and ^{90}Y over the upper 130 m of the water column.

Very little is known about the chemistry of yttrium and more studies are needed but its k_d, representing its affinity for particles, seems to be lower than for Th (*pers. com.* J. Waples). For that reason, with low particle fluxes it will probably be difficult to see $^{90}Y/^{90}Sr$ disequilibrium. The results suggest that the application of $^{90}Y/^{90}Sr$ disequilibria to estimate POC export fluxes is more suitable in higher flux environments. Further work is needed to confirm this hypothesis.

4.3 Modifications and future applications

We want to continue with the improvement of this procedure and studying the potentially valuable tool for examining short-lived episodic particle export events in marine systems that $^{90}Y/^{90}Sr$ disequilibrium could be, due to the short half-life of ^{90}Y of only 64.3 h.

To reduce the processing time we are trying different strategies. The easiest one is to make a precipitate after the first column and filter it instead of evaporate the sample to dryness. Moreover, more test are required but, probably, it can be used an acrylic fiber instead of GF/F filters. With the fibers we only need to prepare all the retention mechanism and then we can leave it working. In addition, if the fibers are impregnated with manganese oxide (MnO_2), they could be used to isolate other radioisotopes of our interest, like actinium or radium, as these elements are scavenged by MnO_2. Thus, different radionuclides from the same sample could be studied at the same time. More testes have to be done in terms to be sure that it works with a good efficiency of extraction and giving better recoveries.

Moreover, in order to avoid overestimates due to the residual yttrium that has not been dragged by the iron hydroxide fifteen days before, the determination of ^{90}Sr could be done extracting it from the water sample by carbonate precipitation or by oxalate extraction (La Rosa *et al.*, 2001; Liong Wee Kwong *et al.*, 2001)

Soon, during three cruises[2] that will take place this year (2009), we will study the disequilibrium between $^{90}Sr/^{90}Y$ in the water column and also, we will collect particle samples from sediments traps and *in* situ filtration pumps to estimate the yttrium in particles and calculate the ratio POC/^{90}Y. All these information will be compared with the data given for the other POC proxies, ^{234}Th and ^{210}Po. The combination of these different tracers is a potential tool that should be used for the determination of the particle dynamics in marine systems over timescales of days (^{90}Y, $T_{1/2}$ = 64.3 h), weeks (^{234}Th, $T_{1/2}$ = 24.1 d) and months (^{210}Po, $T_{1/2}$ = 138.4 d) to improve our understanding of particle dynamics.

Future applications of this method must be done in areas with a high concentration of ^{90}Sr due to the controlled effluent discharges associated with nuclear fuel cycle accidents, losses in the sea and the dumping of nuclear waste (basically from the Shellafield plant) and with low renovation rate of the waters what makes that the amount of particles were high too. Considering this, the Irish or the Baltic Seas could be interesting zones to assay the method and try to learn more about the Y behaviour in relation with particles.

[2] FAMOSO is a Spanish Project funded by the Ministerio de Ciencia y Tecnología that will take place in the NW Mediterranean. The overall objective is to determine the fate of the organic matter of the open sea spring bloom. This project encompasses 3 sampling cruises in 2009, the first one will take place during the bloom (from 6 of February to 23 of March), the second one after the bloom (from 29 of April to 8 of May) and thirst one at the end of the stratification period (from 14 to 21 of September).

5. Conclusions

Although a great deal is known about the carbon cycle, the scientific community is still limited in its ability to make confident predictions about the likely response of the carbon cycle to global environmental change. Oceanic circulation is one of the key processes that control our climate and the use of radionuclides as tracers for oceanic processes could be a useful and valuable tool to study the oceanic particle flux, like has been well demonstrated.

A lot of work needs to be done in order to understand better the behavior of Y in sea water. This project is only the first step for the possible application of ^{90}Y as a new POC proxy. We have to do some tests in places with a higher activity concentration of ^{90}Sr and also with much particle concentration, like the Irish or the Baltic Sea, and it is also important to analyze the ^{90}Y from the particles in order to calculate the ratio POC/^{90}Y, which should be representative of the particles leaving the upper water column, using sediment taps and *in situ* filtration pumps.

From our point of view, ^{90}Y could be a useful tracer of the particle export that takes place in a short time scale (e.g. eddies or storms) and, unlike ^{234}Th and ^{210}Po, it can give us information about the particle flux of determined moments, integrating a time scale of only a few days, or even hours, while the other POC proxies estimated the flux for long periods of time. Therefore, in order to improve our knowledge about POC fluxes in the upper ocean, for future studies we promote the use of ^{90}Sr-^{90}Y coupled with ^{210}Pb-^{210}Po and ^{238}U-^{234}Th has a proxy in seawater and particle samples because we will be able to integrate a wide timescales: days (^{90}Y, $T_{1/2}$ = 64.3 h), weeks (^{234}Th, $T_{1/2}$ = 24.1 d) and months (^{210}Po, $T_{1/2}$ = 138.4 d).

Archer, D., Kheshgi, H., Maier-Reimer, E., 1998. The Dynamics of Fossil Fuel CO2 Neutralization by Marine CaCO3. Global Biochemical Cycles, Vol. 12, pp. 259-276.

Bacon, M.P., Belastock, R.A., Tecotzky, M., Turekian, K.K., Spencer, D.W., 1988. Lead-210 and polonium-210 in ocean water profiles of the continental shelf and slope south of New England. Continental Shelf Research, Vol. 8, Issue 5-7, pp. 841-853.

Benitez-Nelson, C.R., 2008, Annual Report. Collaborative Research: Nitrogen Fixation and its Coupling with Denitrification in the Eastern Tropical North Pacific. USC Research Foundation, United States of America.

Bowen, H.J.M., 1956. Strontium and barium in sea water and marine organisms. Journal of Marine Biology, Vol. 35, pp. 451-460.

Buesseler, K.O., 1991. Do upper-ocean sediment traps provide an accurate record of particle flux? Nature, Vol. 353, pp. 420-423.

Buesseler, K.O., Bacon, M.P., Cochran, J.K., Livingston, H.D., 1992. Carbon and nitrogen export during the JGOFS North Atlantic Bloom Experiment estimated from super ^{234}Th:^{238}U disequilibria. Deep-Sea Research I, Vol. 39, No. 7-8, pp. 1115-1137.

Buesseler, K.O., Benitez-Nelson, C.R., Moran, S.B, Burd, A., Charette, M., Cochran, J.K., Coppola, L., Fisher, N.S., Fowler, S.W., Gardner, W.D., Guo, L.D., Gustafsson, Ö., Lamborg, C., Masqué, P., Miquel, J.C., Passow, U., Santschi, P.H., Savoye, S., Stewart, G., Trull, T., 2006. An assessment of particulate organic carbon to thorium-234 ratios in the ocean and their impact on the application of ^{234}Th as a POC flux proxy. Marine Chemistry, Vol. 100, pp. 213-233.

Burns, N.M, Rosa, F., 1980. In situ measurement of the settling velocity of organic carbon particles and 10 species of phytoplankton. Limnology and Oceanography. Vol. 25, Issue 5, pp. 855-864. American Society of Limnology and Oceanography, Inc.

Bustos-Serrano, H., Castro-Valdez, R., 2006. Flux of nutrients in the Gulf of California: Geostrophic approach. Marine Chemistry, Vol. 99, Issues 1-4, pp. 210-219.

Choppin, G., Liljenzin, J.O., Rydberg, J., 2001. Radiochemistry and nuclear chemistry. Butterworth-Heinemann, 3rd ed., Woburn, United States of America.

Cochran, J.K., Buesseler, K.O, Bacon, M.P., Wang, H.W., Hirschberg, D.J., Ball, L., Andrews, J., Crossin, G., Fleer A., 2000. Short-lived thorium isotopes (^{234}Th, ^{228}Th) as indicators of POC export and particle cycling in the Ross Sea, Southern Ocean. Deep-Sea Research II: Tropical Studies in Oceanography, Vol. 47, Issue 15-16, pp. 3451-3490.

Cochran, J.K., Masqué, P., 2003. Short-lived U/Th Series Radionuclides in the Ocean: Tracers for Scavenging Rates, Export Fluxes and Particle Dynamics. Reviews in Mineralogy & Geochemistry, Vol. 52, pp. 461-492.

De Villiers, S., 1999. Seawater strontium and Sr/Ca variability in the Atlantic and Pacific oceans. Earth and Planetary Science Letters, Vol. 171, Issue 4, pp. 623-634.

Ducklow, H.W., Steinberg, D.K., Buesseler, K.O., 2001. Upper Ocean Carbon Export and the Biological Pump. Oceanography, Special Issue JGOFS, Vol. 14, No. 4, pp. 50-58.

Emerson, S., Stump, C., Johnson, B., Karl, D.M., 2002. In situ determination of oxygen and nitrogen dynamics in the upper ocean. Deep Sea Research Part I: Oceanographic Research Papers, Vol. 49, Issue 5, pp. 941-952.

Fan, S., Gloor, M., Mahlman, J., Pacala, S., Sarmiento, J., Takahashi, T., Tans, P., 1998. A Large Terrestrial Carbon Sink in North America Implied by Atmospheric and Oceanic Carbon Dioxide Data and Models. Science, Vol. 282. No. 5388, pp. 442–446.

Feely, R.A., Sabine, C.L., Takahashi, T., Wanninkhof, R., 2001. Uptake and storage of carbon dioxide in the oceans: The global CO_2 survey. Oceanography 14 (4), 18-32.

Hamilton, T., 2001. Radiation Fallout-Guam. Lawrence Livermore Nacional Laboratory, Technical Information Departament, University of California, Livermore, United States.

Honjo, S., Doherty, K.W., 1988. Large-aperture time-series sediment traps; design objectives, construction and application. Deep Sea Research I. Oceanographic research papers, Vol. 35, No. 1, pp. 133-149.

Houghton, J.T., Jenkins, G.J., Ephraums, J.J., 1990. Climate change: The IPCC scientific. American Scientist, Vol. 80, No. 6, Cambridge University Press Country of Publication, New York, United States.

International Atomic Energy Agency, IAEA, 2005. Worldwide marine radioactivity studies (WOMARS). Radionuclide levels in oceans and seas. Final report of a coordinated research project. IAEA-TECDOC-1429, Vienna, Austria.

Karl, T.R., Trenberth K.E., 2003. Modern Global Climate Change. Science, Vol. 302, Nº. 5651, pp. 1719–1723.

Keeling, R.F., Piper, S.C., Bollenbacher, A.F., Walker, S.J., 2008. Atmospheric CO_2 values (ppmv) derived from in situ air samples collected at Mauna Loa, Hawaii, USA. Carbon Dioxide Research Group. Scripps Institution of Oceanography (SIO), University of California. La Jolla, California USA 92093-0444.
http://cdiac.ornl.gov/ftp/trends/co2/maunaloa.co2

Kershaw, P., Young, A., 1988. Scavenging of ^{234}Th in the eastern Irish Sea. Journal of Environmental Radioactivity, Vol. 6, pp.1-23.

Krivtov, V., Howarth, M.J., Jones, S.E., Souza, A.J., Jago, C.F., 2008. Monitoring and modelling of the Irish Sea and Liverpool Bay: An overview and an SPM case study. Ecological Modelling, Vol. 212, pp. 37-52.

La Rosa, J.J., Burnett, W., Lee, S.H., Gastau, J., Povinec, P.P., 2001. Separation of actinides, cesium and strontium from marine samples using extraction chromatography and sorbents. Journal of Radioactivity and Nuclear Chemistry, Vol. 248, No.3, pp. 765-770.

Le Quéré, C., Rödenbeck, C., Buitenhuis, E.T., Conway, T.J., Langenfelds, R., Gomez, A., Labuschagne, C., Ramonet, M., Nakazawa, T., Metzl, N., Gillett, N., Heimann, M., 2007. Recent Climate Change. Saturation of the Southern Ocean CO2 Sink Due to Recent Climate Change. Science 316, 1735.

Liong Wee Kwong, L., La rosa, J.J., Lee, S.H. Povinec, P.P., 2001. Liquid scintillation spectrometry of beta-emitters in marine samples. Journal of Radioactivity and Nuclear Chemistry, Vol. 248, No.3, pp. 751-755.

Livingston, H.D., 2004. Marine Radioactivity. Radioactivity in the environment. Vol. 6. ELSEVIER Ltd, Oxford, United Kingdom.

Matsumoto, E., 1975. Th-234-U-238 radioactive disequilibrium in the surface layer of the oceans. Geochimica et Cosmochimica Acta, Vol. 39, Issue 2, pp.205-212

Orlandini, K.A., Bowling, J.W., Pinder III, J.E., Penrose, W.R., 2003. ^{90}Y-^{90}Sr disequilibrium in surface waters: investigating short-term particle dynamics by using a novel isotope pair. Earth and Planetary Science Letters 207, pp. 141-150.

Plougl, H., Grossart, H.P., Azam, F., Jørgensen, B.B., 1999. Photosynthesis, respiration, and carbon turnover in sinking marine snow from surface waters of Southern California Bight: implications for the carbon cycle in the ocean. Marine Ecology Progress Series I, Vol. 179, pp. 1-11.

Quay, P.D., Tilbrook, B., Wong, C.S., 1992. Oceanic uptake of fossil fuel CO_2: Carbon-13 evidenve. Science 256, pp. 74-79.

Rutgers van der Loeff, M., Sarin, M.M., Baskaran, M., Benitez-Nelson, C., Buesseler, K.O., Charette, M., Dai, M., Gustafsson, Ö., Masqué, P., Morris, P.J., Orlandini, K., Rodríguez y Baena, A., Savoye, N., Schmidt, S., Turnewitsch, R., Vöge, I., Waples, J.T., 2006. A review of present techniques and methodological advances in analyzing ^{234}Th in aquatic systems. Marine Chemistry 100, pp. 190-212.

Rye, R., Kuo, P.H, Holland, H.D., 1995. Atmospheric carbon dioxide concentrations before 2.2 billion years ago. Nature 378, pp. 603-605.

Santschi, P.H., Li, Y.-H., Bell, J., 1979. Natural radionuclides in the water of Narragansett Bay. Earth and Planetary Science Letters, Volume 45, Issue 1, pp. 201-213.

Sarmiento, J.L., Gruber, N., 2004. Ocean biogeochemical dynamics. http://www.awi.de/fileadmin/user_upload/research/research_divisions/climate_sciences/paleoclimate_dynamics/modelling/lessons/the_global_carbon/sarmientogruber.pdf

Siegel, H., Gerth, M., Heene, T., Ohde, T., Rüß, D., Kraft, H., 2009. Hydrography, currents and distribution of suspended matter during a dumping experiment in the western Baltic Sea at a site near Warnemünde. Journal of Marine Systems, Vol. 75, pp. 397-408.

Siegenthaler, U., Sarmiento J.L., 1993. Atmospheric carbon dioxide and the ocean. Nature 365, pp. 119-125.

Stewart, G., Cochran, J.K., Xue, J., Lee, C., Wakeham, S.G., Armstrong, R.A., Masqué, P., Miquel J.C., 2006. Exploring the connection between ^{210}Po and organic matter in the northwestern Mediterranean. Deep Sea Research Part I: Oceanographic Research Papers, Vol. 54, Issue 3, pp. 415-427.

Stewart, G., Cochran, J.K., Miquel, J.C., Masqué, P., Szlosek, J., Rodríguez y Baena, A.M., Fowler, S.W, Hirschberg, D.J., 2007. Comparing POC export from $^{234}Th/^{238}U$ and $^{210}Po/^{210}Pb$ disequilibria with estimates from sediment tramps in the norhwest Mediterranean. Deep-Sea Research I: Oceanographic Research Papers, Vol. 54, pp. 1549-1570.

Stocker, T.F., Schmittner, A., 1997. Influence of CO_2 emission rates on the stability of the thermohaline circulation. Nature, vol. 388, n°6645, pp. 862-865.

United Nations Scientific Committee on the Effects of Atomic Radiation, UNSCEAR, 1993. Sources and effects of ionizing radiation. Annex B: Exposures from man-made sources of radiation, pp. 91-120. United Nations, New York, United States of America.

Verdeny, E., Masqué, P., Maiti, K., Garcia-Orellana, J., Bruach, J.M, Mahaffey, C., Benitez-Nelson, C.R, 2008. Particle export within cyclonic Hawaiian lee eddies derived from ^{210}Pb–^{210}Po disequilibrium. Deep-Sea Research II, Vol. 55, pp. 1461– 1472.